

Measurement and Analysis of the Fluctuations and Poloidal Flow on JFT-2M Tokamak

K. Hoshino 1), T. Ido 2), Y. Nagashima 3), K. Shinohara 1), H. Ogawa 1), K. Kamiya 1), H. Kawashima 1), K. Tsuzuki 1), Y. Kusama 1), K. Ohasa 1), K. Uehara 1), S. Kasai 1), Y. Hamada 2), A. Ejiri 4), Y. Takase 4) and JFT-2M Group 1)

- 1) Japan Atomic Energy Agency, Naka, Japan
- 2) National Institute for Fusion Science, Toki, Japan
- 3) Kyushu Univ., Fukuoka, Japan
- 4) The Univ. Tokyo, Tokyo, Japan

e-mail contact of main author: hoshino.katsumichi@jaea.go.jp

Abstract. The recent studies on potential/density fluctuations and poloidal flow in the JFT-2M tokamak are reported. In the ohmic heated (OH) elongated plasma and in the L-mode plasma, we observe a marked characteristic electrostatic oscillation in the fluctuation spectrum, a GAM (Geodesic Acoustic Mode), which is a kind of a zonal flow, in the plasma edge region ($0.7a \sim 1.0a$, a is the minor radius of the outmost magnetic surface). The detailed structure of the potential and electric field of the GAM was identified by the heavy ion beam probe (HIBP) measurement. The GAM seemed to have an eigen-mode structure. On the study of the generation mechanism, the bispectrum function was estimated by analyzing the reciprocal Langmuir probe (RLP) data, and it was found that the GAM has a significant nonlinear three-wave coupling between the background turbulence. We observe a significant nonlinear coupling (cross bicoherence) between the potential fluctuations and density fluctuations by analyzing the HIBP data. The GAM disappears after the H-mode transition, presumably due to the weakening of the turbulent drive; the potential/density fluctuation power decreases about one order. Instead negative DC electric field dominates at the edge transport barrier (ETB) during the H-mode (by ECH as well as by NBH). The estimated $E \times B$ DC poloidal flow at the ETB in the H-mode is found to be typically 10~20 times larger than the oscillating (~ 15 kHz) poloidal flow by the GAM in the L-mode. By the application of the edge ECH to NBH L-mode, low frequency potential fluctuation is found to increase accompanied by GAM, and at the L-H transition, the GAM is found to exist for a short time (for ~ 10 ms) even after the transition but disappears soon. The low frequency oscillation (< 5 kHz) dominates during the H-mode. We observe a few characteristic potential oscillations (0.3kHz to 1kHz) which are marked during the H-mode, and disappears at the occurrence of the ELM. Multi-mode (100kHz~200kHz) appears in the potential/density fluctuations in the ELM-free phase. In the “H”-phase”, which is an enhanced D_α quasi-steady ETB phase, a quasi-coherent mode (50kHz~100kHz) appears in the potential/density fluctuations which seems to act for maintaining the steady ETB by slightly degrading the transport by reducing the radial electric field.

1. Introduction

In the research, aiming at the realization of the thermonuclear fusion reactor, it was very lucky that the confinement of the tokamak plasma has been found to improve by itself by forming the edge transport barrier (ETB) [1] or by the internal transport barrier (ITB) [2]. Since the plasma fluid can contain various oscillations and cooperative phenomena (instabilities, turbulences) by the electromagnetic interactions, it is very difficult to fully understand the transport in such a complex system, and we have not come to the full understanding. But recent studies on the transport progressed to reveal the importance of the structure of the electric field, magnetic curvature and plasma flow in the plasma interior. It is found that by the formation of the transport barriers, the fluctuation level decreases and the fluctuation induced particle/ heat flux, which is called the anomalous transport [3] which adds to the neoclassical collisional transport [4], decreases. Recently, the potential/ density fluctuations of the tokamak plasma draw much attention in their close relation with the “zonal flow” [5] which is a localized poloidal flow considered to decrease the plasma turbulent (anomalous) diffusion and considered as a candidate of the mechanism of the transport barrier. The turbulence generates the zonal flow and the zonal flow suppresses the turbulence. The

stationary state is considered to be decided by the balance of these mechanisms. There are two kinds of the zonal flow, one is stationary and the other is oscillatory. The stationary zonal flow is considered to have mode number $m/n=0/0$ with frequency 0, and difficult to detect. The oscillatory zonal flow is called as “geodesic acoustic mode (GAM)” generated by the geodesic curvature of the confining magnetic field [6].

In the JFT-2M tokamak, potential/ density fluctuations, GAM, spatial structure of the potential, radial electric field and resultant poloidal flow have been studied in the ohmically heated (OH) plasma and additionally heated plasma (L-mode, H-mode) by the electron cyclotron heating (ECH) and neutral beam heating (NBH).

The contents of the paper are as follows, the experimental set-up is described in Sec.2, the experimental results and discussions are described in Sec.3. A summary is given in Sec.4

2. Experimental set-up

JFT-2M [7] is a tokamak with non-circular cross section with major radius $R_0=1.31\text{m}$, minor radius $a=0.35\text{m}$, maximum elongation $\kappa=1.7$ and maximum toroidal field at the plasma center $B_{t0}=2.2\text{T}$. The frequency of the ECH system is 60GHz with movable k_{\parallel} antenna [8]. A hydrogen 40keV NBH system consists of two oblique beams (co-beam and counter beam) with the typical injection angles of about 40 deg.s (toroidal) from the perpendicular injection and 4.8 deg.s (poloidal) from the horizontal injection [9].

The spatial structure of the potential/density and their fluctuations were measured by the heavy ion ($_{81}\text{Tl}^+$, Thallium) beam probe (HIBP) [10]. A fast moving ($\sim 1\text{mm}/1\text{ms}$) reciprocate Langmuir probe (RLP) [11] which has four electrodes measured the profiles and fluctuations of edge potential, saturation currents, and temperatures. An O-mode microwave reflectometer (MRM) [12] ($f = 38\text{GHz}$, 28GHz) was also used to measure the density fluctuations at electron density of $n_e = 1.8 \times 10^{19}\text{m}^{-3}$, $0.97 \times 10^{19}\text{m}^{-3}$.

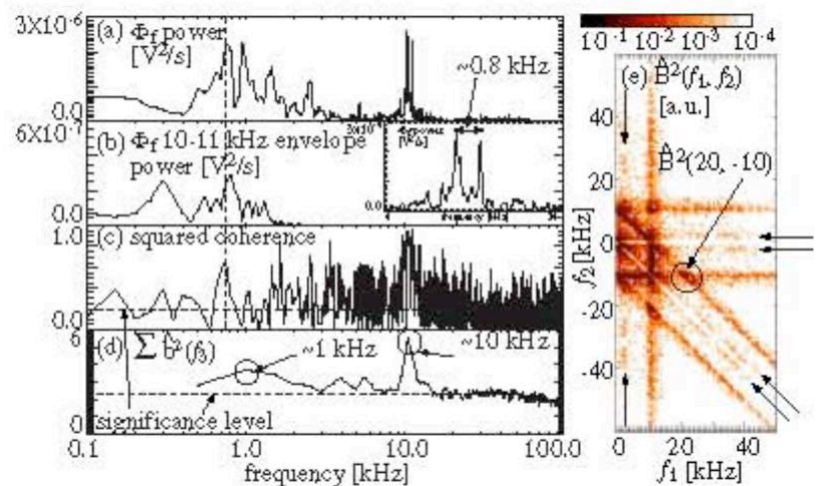


FIG.1 Potential spectrum and bicoherence measured by the RLP in the OH plasma. (Reprinted from Ref.11)

3. Experimental Results and Discussions

3.1 Nonlinear interaction of GAM with the background turbulence in the OH plasma

The power spectrum of the potential fluctuations in the elongated OH plasma (in the limiter discharges as well as in the divertor discharges) was typically found to consist of several characteristic peaks (FIG.1), a high frequency coherent mode ($f_H = 10 \sim 20\text{kHz}$), and low frequency modes (LFM, $\sim 1\text{kHz} < f_L < \sim 4\text{kHz}$) and background turbulent oscillations, at the plasma edge ($0.9a < r < 1.0a$, where a is the minor radius at the position of the outmost magnetic surface) by the RLP as well as the by the MEM. From the poloidal long correlation of the high frequency electrostatic oscillation f_H , and its frequency compared to the theoretical GAM

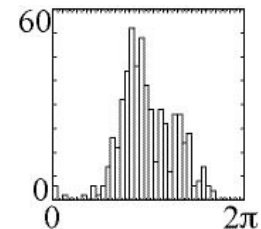


FIG.2 histogram of the biphase at the GAM frequency.

EX/2-2

frequency $f_{GAM} \sim \frac{c_s}{2\pi R}$, where c_s is the sound velocity, using the measured edge temperature, the high frequency peak was considered to be the GAM [11]. The LFM is not the GAM by the consideration of their frequencies (too low). The background potential turbulence behaved as the drift-wave-like; the measured fluctuations satisfy the relation of $\tilde{n}_e/n_e \approx \tilde{\phi}/T_e$, and the cross coherence of \tilde{n}_e and $\tilde{\phi}$ was significant $\langle \tilde{n}_e, \tilde{\phi} \rangle \sim 0.7$. The total

(summed) squared bicoherence $\sum_{f_2} b^2(f_1, f_2) = \sum_{f_2} \frac{|\hat{B}(f_1, f_2)|^2}{\langle |\Phi(f_1, f_2)|^2 \rangle \langle |\Phi(f_3)|^2 \rangle}$ between the

background turbulence and the GAM was estimated and the significant nonlinear three wave interaction between them was found. Here \hat{B} is the bispectrum function of the Fourier component $\Phi(f)$ of $\phi(t)$; $\hat{B}(f_1, f_2) = \langle \Phi(f_1)\Phi(f_2)\Phi^*(f_3 = f_1 \pm f_2) \rangle$. The power of the GAM oscillation was found to be proportional to the bicoherence, which showed the possibility that the GAM is generated by the nonlinear interaction of the background turbulence. Further, the biphas

$\theta = \tan^{-1} \frac{\text{Im} \hat{B}(f_1, f_2)}{\text{Re} \hat{B}(f_1, f_2)}$, was estimated [13]. The obtained

biphase of the GAM frequency was concentrated around $\sim 0.8\pi$ (FIG.2), but the biphase between the turbulent waves was randomly distributed, in consistent with a theoretical picture on the drift wave-zonal flow system [14]. In the process of the bicoherence analysis, we found that the value

of the bicoherence almost linearly increased as the inverse of the realization number, and the realization number needed for the good convergence of the bicoherence value amounted to several hundreds (FIG.3) [15]. The typical value of the converged total bicoherence was ~ 0.9 for the GAM whereas ~ 0.05 for the background turbulence. As stated above, we find LFMs ($f_L \sim 1\text{kHz}$) other than the GAM ($f_H \sim 10\text{kHz}$). The nonlinear coupling of the GAM and background turbulence is clear (FIG.1). We also observed a nonzero bicoherence between the LFMs (f_L) and the background turbulence. Therefore, it is found that a weak nonlinear interaction exists between the turbulence and the LFM as well as between the turbulence and the GAM.

3.2 Identification of the potential structure of the GAM and interaction with the density fluctuations in the L-mode plasma

The GAM is also observed during the L-mode [16,17,18]. The potential structure of the GAM was identified by the HIBP measurement. The amplitude of the potential has a peak value of $\phi \sim 15\text{V}$ at $\sim 3\text{cm}$ inside of the separatrix with the full half width of $\sim 4\text{cm}$. The frequency of the GAM f_{GAM} was found to be fairly constant ($\sim 15\text{kHz}$) in space in spite of the spatial change of the temperature. The GAM is considered to be a radially propagating wave and has an eigenmode-like structure.

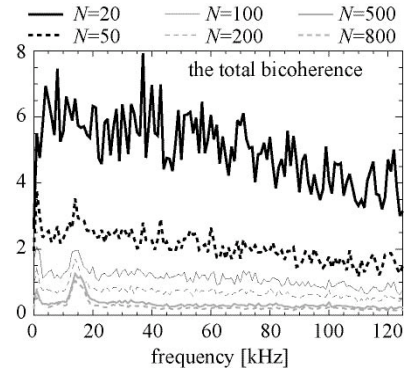


FIG.3 Convergence of the total bicoherence with realization number N .

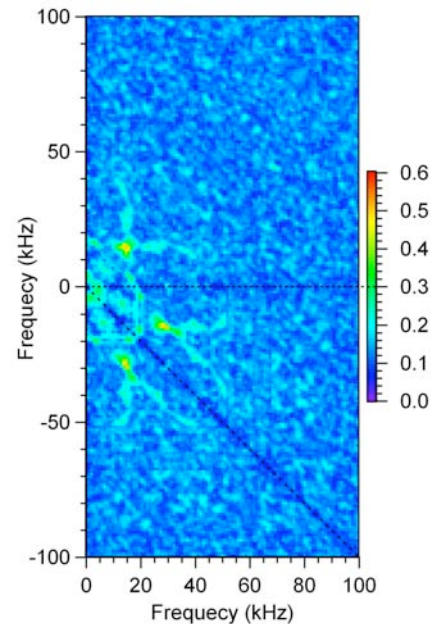


FIG.4a Autobicoherence ($\phi\phi\phi$) of the potential fluctuation by HIBP at $r \sim 0.9a$ during the L-mode.

The Boltzmann relation between \tilde{n}_e , $\tilde{\phi}$ was satisfied at the peak of the GAM potential. An interaction of the GAM with ambient density fluctuation was observed. The modulation of the envelope of the density fluctuation $|\tilde{n}_e|$ with f_{GAM} (not $2f_{GAM}$) is not explained by the conventional turbulence suppression by the shear flow. A theory which takes a dynamic shearing effect into account [19,20], and which is related to $\frac{\partial \tilde{V}_{E \times B}}{\partial r}$, is considered to be consistent with the observation [18]. The observed frequency and the modulation fraction of the ambient density fluctuation (~ 0.2) was in good agreement with the theory. Figure 4a shows the autocorrelation of the potential measured by HIBP during the L-mode. Though the obtained bicoherence is not very large, nonzero three-wave interaction between the GAM ($f_H \sim 15\text{kHz}$) and the background turbulence ($0\text{ kHz} < f < \sim 40\text{kHz}$) is observed. Figure 4b shows the crossbicoherence between the density fluctuation and potential fluctuation from the HIBP data. We observe a nonzero nonlinear coupling between the turbulence density fluctuation and GAM potential fluctuation. Also we find a nonlinear coupling between the turbulence and the LFM.

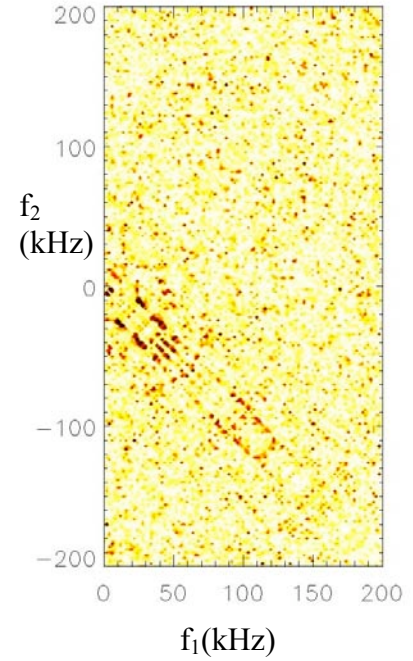


FIG.4b Crossbicoherence ($nn\phi$) of the density fluctuation and potential fluctuation by HIBP at $r \sim 0.9a$ during the L-mode.

3.3 Fluctuations and ExB flow during the H-mode

3.3.1 Disappearance of the GAM In the H-mode, the power level of the potential/density fluctuation decreases by an order of magnitude in the high frequency region ($\geq \sim 3\text{kHz}$) and apparently the GAM ($\sim 15\text{kHz}$) disappears (FIG.5). The GAM growth rate may be decreased because of the decrease of the background turbulence level during the H-mode.

3.3.2 Comparison of the radial electric field and ExB poloidal flow during the H-mode and by the GAM during the L-mode

The H-mode has been produced solely by edge ECH in JFT-2M since 1989 [21]. We measured a negative radial electric field $E_r \sim -140\text{ V/cm}$ and resultant $E \times B$ poloidal flow by the HIBP measurement (FIG.6) during the ECH H-mode. If the enhanced trapped electron

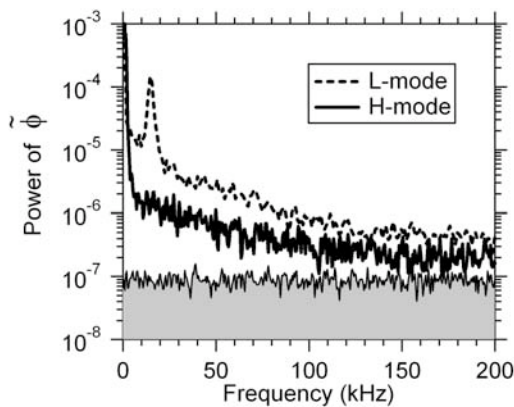


FIG.5 Comparison between the typical potential spectrum of L-mode and H-mode during NBH (HIBP).

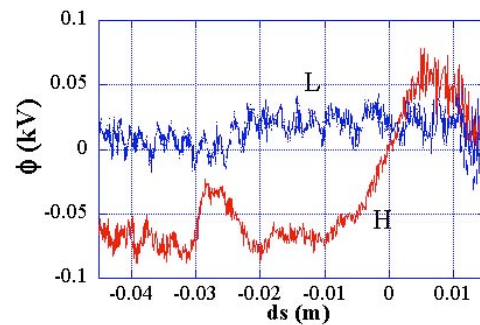


FIG.6 Potential profile measured by the HIBP during the ECH H-mode and ECH L-mode. $I_p = 0.23\text{MA}$, $B_{10} = 1.23\text{T}$, ECR layer at $0.86a$, $P_{EC} = 0.37\text{MW}$. Upper single null configuration. ds is a distance from the separatrix

loss by ECH dominates, the resultant E_r should be positive, therefore it is clear that this effect does not contribute to the production of the negative E_r . This E_r is the same level with the NBH H-mode (typically $\sim 200\text{V/cm}$). The negative radial electric field $E_r \sim -130\text{V/cm}$, and positive $E_r \sim 40\text{V/cm}$ develops quickly. The estimated \mathbf{ExB} poloidal flow changes its direction between the ETB $v_{p,ExB} \sim -12\text{km/s}$ and scrape off layer (SOL) $v_{p,ExB} \sim +4\text{km/s}$. Therefore, a large flow velocity shear $\sim 1.6 \times 10^6/\text{s}$ was found to exist at the separatrix. The DC flow during the H-mode is found to be typically 10~20 times larger than the oscillating \mathbf{ExB} flow by the GAM ($\sim 15\text{kHz}$, $5\sim 10\text{V/cm}$) during the L-mode.

3.3.3 Spectra of the low frequency electrostatic oscillations during the H-mode by NBH and with ECH

As already shown in FIG.5, the power of the electrostatic fluctuation concentrates in the low frequency region. At the L/H transition by NBH, an increase of the low frequency potential fluctuation ($\sim 0.3\text{kHz} < f < \sim 1\text{kHz}$) was observed as well as at the H/L back transition [22]. During the H-mode, the low frequency mode around $f \sim 1\text{kHz}$ and $f \sim 0.3\text{kHz}$ was evident.

Figure 7 shows the case of the L/H transition by the ECH of the NBH heated L-mode plasma. The H transition occurs at $t \sim 740\text{ms}$. By the application of the

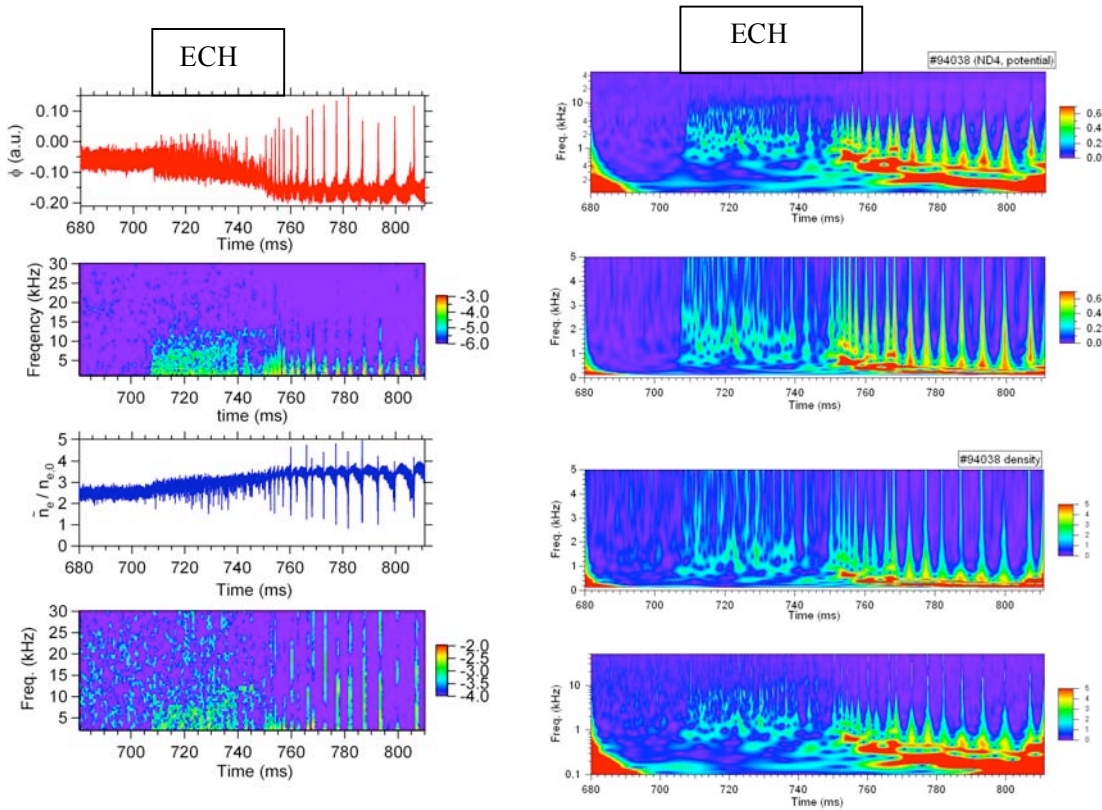


FIG.7 H-mode transition by ECH of the NBH L-mode. (left) potential ϕ , FFT spectrum of ϕ , density fluctuation and FFT of them. (right) Wavelet spectra of ϕ and density fluctuation in the range of 0-20kHz, and 0-4kHz. $P_{NB}=0.30\text{MW}$, $P_{EC}=0.20\text{MW}$. $I_p=0.21\text{MA}$. $B_{i0}=1.20\text{T}$. $\beta_p=0.39$. $\kappa=1.46$. $\delta=0.46$. $\bar{n}_e = 1.8 \times 10^{19}\text{m}^{-3}$ before the ECH injection (L-mode), \bar{n}_e increased by the H transition up to $2.8 \times 10^{19}\text{m}^{-3}$ at $t=820\text{ms}$ (H-mode).

ECH, the low frequency potential fluctuation $\tilde{\phi}$ below 10kHz increases with the GAM-like structure around 10kHz. The potential drop begins from 735-740ms somewhat slower than the NBH case, and the potential/density fluctuations are suppressed. It is found that the GAM-like structure survives at the L/H transition ($t=740\text{ms}-750\text{ms}$). At $t=750\text{ms}$ to 755ms , an increase of the low frequency oscillation is found and the potential drop becomes stationary. The increase of the fluctuation is similar to the NBH case. After the ECH, ELMy H-mode continues with NBH. Between the ELMs, we aware weak relatively broad band potential fluctuations around $f=0.5\text{kHz}$ to 5kHz . If one assumes any $m > 1$ poloidal irregularity of the \mathbf{ExB} flow, we may be able to estimate the frequency by $V_{p,ExB}/2\kappa\pi a > \sim 12[\text{km/s}]/\sim 2m = 6\text{kHz}$. The observed frequency structure is lower. Therefore if the zonal flow exists in the ETB and if it affects the potential fluctuations, such low frequency potential fluctuation might be a candidate of the effect of the zonal flow. But still we could not identify that the dominant mode number of the LFM is $m/n=0/0$ or not. Also, we still have not observed any significant bicoherence in the potential/density fluctuations during the H-mode.

3.3.4 Spectra of the high frequency characteristic modes during the H-mode (ELM-free, H', EDA(HRS) –like phase)

During the ELM-free H-mode phase (FIG.8), we find “multiple modes” ($100\text{kHz} < f < 200\text{kHz}$), which has electrostatic nature (not very clear in the magnetic probe signal), appears in the ETB. The modes have almost equal frequency spacing of $\Delta f \sim (18\sim 20)\text{kHz}$. If we assume that the difference comes from the difference in the toroidal mode number, the component of the $n=7$ to 11 is strong. It has some features of the drift ballooning mode [24] that only such high mode numbers are unstable. The shear parameter $s=2\sim 3$, pressure parameter $\alpha=2\sim 3$, and magnetic Reynolds number $S = (0.5\sim 1)\times 10^5$ are similar to their assumptions.

These multi-modes seem to cascade (decrease of the toroidal mode number) to a single lower frequency quasi-coherent mode (QCM, $n\sim 1$) in the H'-phase [25], in which phase a slight degradation of the confinement occurs compared to the ELM-free phase. The spectrum in the QCM region ($50\text{kHz} < f < 80\text{kHz}$) is different from spectrum during the ELM-free H-mode [23]. The HIBP measurement revealed that the QCM exist in the ETB ($0\text{ cm} < r < 2\text{ cm}$ inside of the separatrix) and the $E_r \sim -80\text{V/cm}$ is about 40% of $E_r \sim -200\text{V/cm}$ at the ELM-free phase [23]. Therefore the QCM seems to enhance the transport by decreasing the $|E_r|$, and the ETB seems to be maintained stationary with decreased gradient.

In the high recycle phase during which the D_α line intensity increases (called as EDA [26]-like or HRS [27]), the magnetic fluctuation \tilde{B}_p becomes stronger and the typical toroidal mode number was identified $n=1$ (QCM 46kHz) to 7 (320kHz) [28]. The power concentrated in $n=5$ to 8 peaked at $n=7$ in the high frequency region.

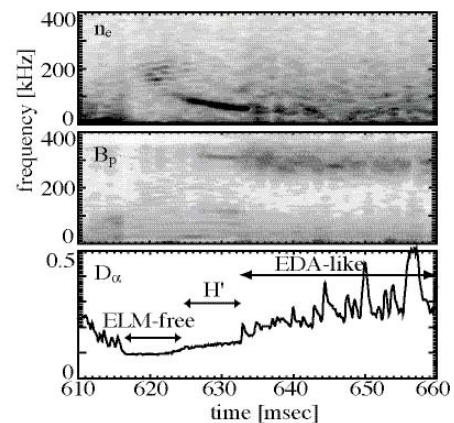


FIG.8 Density fluctuation by MRM (upper), magnetic fluctuation (middle) and D_α signal (lower) in the H-mode by NBH. The electrostatic multi modes during the ELM free phase and the QCM during the H' phase are evident. (Reprinted from [23])

EX/2-2

4. Summary

- 1) The GAM is found in the OH phase, L-mode phase and at the beginning of the H-mode. The potential structure of the GAM was identified. The GAM behaves as an eigen mode.
- 2) The three wave coupling between the background turbulent potential oscillations and GAM was clarified. A weak nonlinear coupling was observed between the background turbulent oscillations and the low frequency modes.
- 3) The structure of the potential profile was measured during the ECH H-mode, and negative electric field and resultant DC poloidal flow were clarified and the poloidal velocity was found to be 10~20 times larger compared with the typical AC poloidal flow by the GAM.
- 4) A low frequency (< 5 kHz) potential fluctuation is observed during the H-mode. This may be a candidate of the stationary zonal flow but we could not identify the mode number yet.
- 5) Characteristic modes appear such as Multi-modes during the ELM-free H-mode and quasi-coherent mode (QCM) during the enhanced D_α H-mode (H' mode). The QCM exists in the ETB and reduces the radial electric field $|E_r|$ which may cause the degradation of the transport and maintains the ETB.

Acknowledgments

The authors are grateful to Dr. Y. Miura of the Japan Atomic Energy Agency, Dr. A. Nishizawa of the National Institute for Fusion Science, and Dr. S. Kanazawa of the Ibaraki Univ. for their contribution to the HIBP measurement. They are also grateful to Prof. K. Itoh, Prof. S. I. Itoh, and Prof. A. Fujisawa for their useful discussions on the zonal flow and GAM. The main author is grateful to the late Dr. H. Maeda who made much efforts to introduce the innovative diagnostics to the JFT-2M in the cooperative research with the universities and the institutes, with these innovative diagnostics the physical understanding of the tokamak plasma has much progressed in the JFT-2M tokamak in time before the shut-down.

References

- [1] F.Wagner et al., "Regime of Improved Confinement and High Beta in Neutral-Beam-Heated Divertor Discharges of the ASDEX Tokamak", *Phys. Rev. Lett.* **49**, 1408 (1982).
- [2] Y.Koide et al., "Internal Transport Barrier on $q=3$ Surface and Poloidal Plasma Spin up in JT-60U High β_p Discharges", *Phys. Rev. Lett.* **72**, 3662 (1994).
- [3] J.W.Connor and H.R.Wilson, "Survey of theories of anomalous transport", *Plasma Phys. Control. Fusion* **36**, 719 (1994).
- [4] F.L.Hinton and R.D.Hazeltine, "Theory of plasma transport", *Rev. Mod. Phys.* **48**, 239 (1976).
- [5] P.H.Diamond et al., "Review of Zonal Flows", *Plasma Phys. Control. Fusion* **47**, R35 (1994).
- [6] N.Winsor et al., "Geodesic Acoustic Waves in Hydromagnetic Systems", *Phys. Fluids* **11**, 2448 (1968).
- [7] "Special issue on JFT-2M Tokamak", *Fusion Sci. & Tech.* **49** (2) (2006).
- [8] K.Hoshino et al., "Suppression of the $m/n = 2/1$ tearing mode by ECH/ECCD on JFT-2M Tokamak", *Fusion Eng. Design* **53**, 249 (2001).
- [9] K.Hoshino et al., "Heating, current drive, and advanced plasma control in JFT-2M", *Fusion Sci. & Tech.* **49**, 139 (2006).
- [10] T.Ido et al., "Observation of the Fast Potential Change at L-H Transition by a Heavy-Ion-Beam Probe on JFT-2M", *Phys. Rev. Lett.* **88**,055006-1 (2002).
- [11] Y. Nagashima et al., "Observation of Nonlinear Coupling between Small-Poloidal Wave-Number Potential Fluctuations and Turbulent Potential Fluctuations in Ohmically Heated Plasmas in the JFT-2M Tokamak", *Phys. Rev. Lett.* **95**, 095002 (2005).

- [12] K. Shinohara et al., “A New Method to Analyze Density Fluctuation by Microwave Reflectometry” *Jpn. J. Appl. Phys.* **36**, 7367 (1997).
- [13] Y. Nagashima et al., “Bispectral analysis applied to coherent floating potential fluctuations obtained in the edge plasmas on JFT-2M”, *Plasma Phys. Control. Fusion* **48**, S1 (2006).
- [14] K. Itoh et al., “On the bicoherence analysis of plasma turbulence”, *Phys. Plasmas* **12**, 102301 (2005).
- [15] Y. Nagashima et al., “Convergence study of bispectral analysis in experiments of high temperature plasmas”, *Rev. Sci. Instrum.* **77**, 045110 (2006).
- [16] T. Ido et al., “Electrostatic fluctuation and fluctuation induced particle flux during formation of the edge transport barrier in the JFT-2M tokamak”, in *Proc. IAEA Fusion Energy Conf. 2004, EX/4-6Rb* (2004).
- [17] T. Ido et al., “Observation of the interaction between the geodesic acoustic mode and ambient fluctuation in the JFT-2M tokamak”, *Nucl. Fusion* **46**, 512 (2006).
- [18] T. Ido et al., “Geodesic-acoustic-mode in JFT-2M tokamak plasmas”, *Plasma Phys. Control. Fusion* **48**, S41(2006).
- [19] K. Hallatschek et al., “Transport Control by Coherent Zonal Flows in the Core/Edge Transition Regime”, *Phys. Rev. Lett.* **86**, 1223 (2001).
- [20] K. Itoh et al., “Excitation of geodesic acoustic mode in toroidal plasmas”, *Plasma Phys. Control. Fusion* **47**, 451(2005).
- [21] K. Hoshino et al., “H Mode Observed in the JFT-2M Tokamak with Edge Heating by Electron Cyclotron Waves”, *Phys. Rev. Lett.* **63**, 770 (1989).
- [22] T. Ido et al., in *Workshop on confinement and transport* (2005).
- [23] K. Hoshino et al., “On MHD Oscillations in High Beta H-Mode Tokamak Plasma in JFT-2M”, *J. Plasma Fusion Res. SERIES*, **Vol.6**, 345 (2004).
- [24] R. J. Hastie et al., “Drift ballooning instabilities in tokamak edge plasmas”, *Phys. Plasmas* **10**, 4405 (2003).
- [25] K. Shinohara et al., “Density Fluctuations in the JFT-2M H-Mode Plasma Measured by Using a New Analysis Method of Microwave Reflectometry”, *J. Plasma Fusion Res.* **74**, 607 (1998)
- [26] M. Greenwald et al., “Characterization of enhanced D_{α} high-confinement modes in Alcator C-Mod”, *Phys. Plasmas* **6**, 1943 (1999)
- [27] K. Kamiya et al., “Observation of High Recycling Steady H-mode edge and compatibility with improved core confinement mode on JFT-2M”, *Nucl. Fusion* **43**, 1214 (2003).
- [28] K. Kamiya et al., “High recycling steady H-mode regime in the JFT-2M tokamak”, *Plasma Phys. Controlled Fusion* **46**, A157 (2004).